Periodicity-enhanced structures for efficient sound absorption

V.V. Krylov[1], A. Azbaid El Ouahabi[1]
[1] Department of Aeronautical and Automotive Engineering, Loughborough University, Loughborough, Leicestershire LE11 3TU, UK
e-mail: **V.V.Krylov@lboro.ac.uk**

Abstract

In the present work, an overview of experimental investigations of the two types of periodicity-enhanced acoustic absorbing structures is given. In the first type of structures, the performance of acoustic absorbing materials is improved by providing a smooth transition from the impedance of air to the impedance of the absorbing material in question. This smooth change in the impedance is materialised using gradient index metamaterial layers formed by quasi-periodic arrays of solid cylinders. In the second type of performance improving devices, the principle of acoustic black holes has been implemented. To achieve the required power-law decrease in sound velocity with propagation distance the cylindrical inhomogeneous acoustic waveguides enhanced by quasi-periodic systems of concentric rings have been used. Measurements of the reflection coefficients for both types of structures have been carried out. The results show the possibility of substantial reduction of the acoustic reflections in both cases.

1 Introduction

In this work, an overview of the recent experimental research into the two types of periodicity-enhanced acoustic absorbing structures is presented. In the first type, the performance of acoustic absorbing materials is improved by providing a smooth transition from the impedance of air to the impedance of the absorbing material in question. This smooth change in the impedance is materialised via application of gradient index metamaterial layers formed by quasi-periodic arrays of solid cylinders (brass tubes) with their external diameters gradually increasing from the external row of tubes facing the open air towards the internal row facing an absorbing porous layer. If acoustic wavelengths are much larger than the periodicity of the array, such a structure provides a gradual increase in the acoustic impedance towards the internal row of cylinders, thus providing the possibility of almost perfect impedance matching between the air and porous absorbing materials, such as foams, sponges, etc. Measurements of sound reflection coefficients have been undertaken for different types of absorbing materials in combination with the relevant numbers of rows of brass cylinders to achieve the required impedance matching. The results show that the presence of matching metamaterial layers brings substantial reduction in the sound reflection coefficients, thus increasing the efficiency of sound absorption.

In the second type of performance improving devices, the principle of acoustic black holes has been implemented. To achieve the required power-law decrease in sound velocity with propagation distance the cylindrical inhomogeneous acoustic waveguides enhanced by quasi-periodic systems of concentric rings have been used. Measurements of the reflection coefficients for guided acoustic modes incident on such black holes have demonstrated the possibility of substantial reduction of the acoustic reflections even without insertion of any absorbing materials.

The paper is organised as follows. Initially, the investigations of the metamaterial structure, called 'Quasi-flat acoustic absorber' is described. Then, the waveguiding quasi-periodic structure implementing the acoustic black hole is considered. Finally, the conclusions are drawn to summarise the findings.

2 Quasi-flat acoustic absorbers enhanced by metamaterial layers

Like metamaterials in other areas of physics, acoustic metamaterials gain their properties from structure rather than composition, using the inclusion of small inhomogeneities to achieve desirable macroscopic behavior [1-3]. As one of the recent examples of such metamaterials one can mention periodic arrays of acoustic black holes for flexural waves that provide efficient vibration damping [4, 5]. In some recent publications (see e.g. [6-8]) the attention has been paid to the design of cylindrical or spherical omnidirectional sound absorbers using acoustic metamaterials for gradual impedance matching between the air and the absorbing core.

In this section, we describe the results of the recent investigations of the acoustic absorbing structure, the "Quasi-Flat Acoustic Absorber" (QFAA), enhanced by the presence of gradient metamaterial layers [9, 10]. A typical example of such a device consists of an absorbing layer and a quasi-periodic array of solid cylinders (brass cylindrical tubes) with their filling fractions varying from the external row facing the open air towards the internal row facing the absorbing layer made of a porous material. A gradient metamaterial layer formed by such cylinders is used to gradually adjust the impedance of the air to that of the porous absorbing material and thus to reduce the reflection. Two types of common porous absorbers (Sponge and Fiberglass) have been tested to demonstrate the importance of matching the effective acoustic impedance at the exit of the metamaterial layer to that of the porous material. All the brass tubes are of the same length (305 mm) and arranged as a rectangular array placed into a wooden box with the dimensions of 569 x 250 x 305 mm. The designed structure was manufactured and experimentally tested in an anechoic chamber at the frequency range of 500 – 3000 Hz.

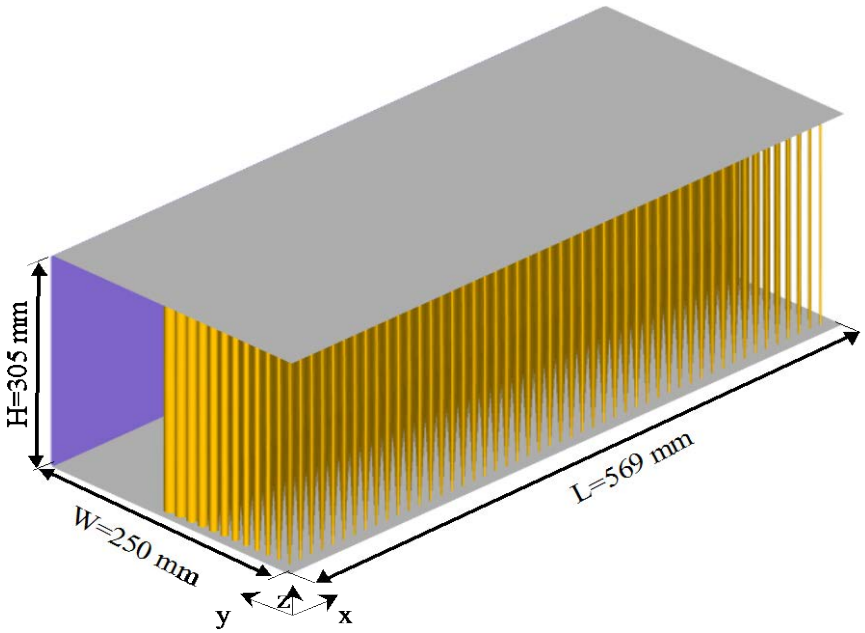

Figure 1: Schematic 3D view of a Quasi-Flat Acoustic Absorber (QFAA) showing the absorbing material zone (on the back) and the impedance matching metamaterial layer formed by a quasi-periodic array of Brass cylinders.

2.1 Experimental setup and methodology

A wooden box with the dimensions of 569x250x305 mm was designed with two zones, one for the impedance matching metamaterial and the other - for a porous absorbing material. The zone of matching metamaterial was drilled in opposite sides to accommodate an array of Brass tubes with the diameters gradually increasing from the external row facing the open air towards the internal row facing the absorbing material. The tubes were arranged in 12x51 pattern with the square lattice constant a = 11 mm.

Figure 1 shows a 3D schematic view of the Quasi-Flat Acoustic Absorber (QFAA). The 305 mm long Brass cylinders (tubes) had the increasing external diameters D_n = 1.6 mm + (n-1)·0.8 mm, where n is the row number, Thus, the Quasi-Flat Acoustic Absorber consists of a system of solid cylinders with varying filling fraction backed by a layer of the absorbing material.

Filling fraction ff and effective acoustic impedance Z_{eff} are defined as follows [8]:

$$ff = \pi\left(\frac{D}{2a}\right)^2, \tag{1}$$

$$Z_{eff} = Z_0 \frac{\sqrt{1+ff}}{1-ff}, \tag{2}$$

where D is the diameter of the cylinders and Z_0 = 413 Rayl is the impedance of air. The calculated effective impedance defined by equation (2) and normalized to the impedance of air is shown in Figure 2 as a function of a row number *n*.

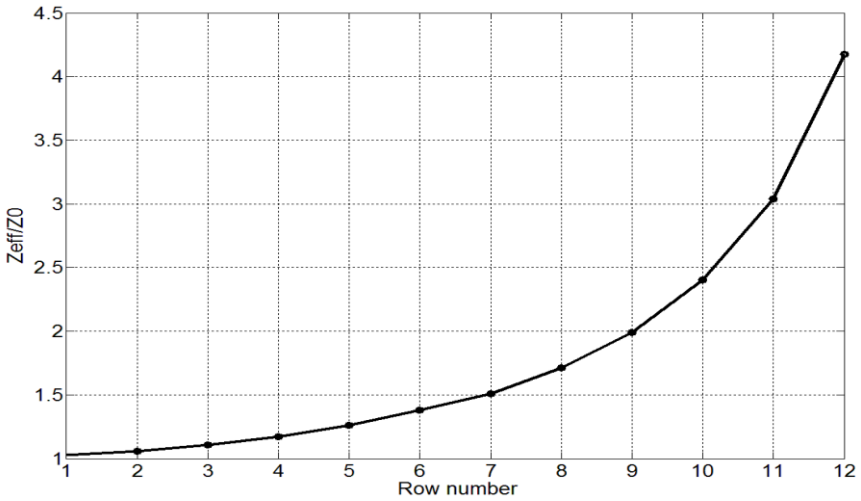

Figure 2: Normalized effective impedance of the metamaterial layer as a function of a row number.

The experiments have been carried out in the anechoic chamber of the Department of Aeronautical and Automotive Engineering at Loughborough University. As a sound source, a loudspeaker was used. It was

suspended on a pulley system that allowed its center to be located at 853 mm height above ground. The centre of QFAA surface was aligned with the loudspeaker and placed at 2 m from the source in order to produce the desired almost plane wave fronts when the sound reaches the sample.

Figure 3: Photograph of the experimental set up showing the QFAA (left) and the loudspeaker (right).

Two G.R.A.S. 40AE, pre-polarized ½ inch free-field microphones (their sensitivities are 44 mV/Pa (Mic1) and 42 mV/Pa (Mic2)), with G.R.A.S. preamplifiers type 26CA, were used to measure sound pressure. Figure 3 shows the photograph of the experimental set up utilised to measure the sound pressure reflection coefficients. Two methods of measuring the sound pressure reflection coefficients have been used: the traditional Standing Wave Ratio method (SWR) and the Two Microphone Transfer Function Method (TFM). In the latter case, a white noise generator was used to drive the loudspeaker. Two microphones have been used to measure sound pressure, and a computer program was used to compute the transfer function between two microphone positions and then calculate the reflection coefficient from the sample. The distance from the sample face to the first microphone was 155 mm, and the distance between the microphones was 35 mm. The microphones were connected to a PC via a four-channel dynamic signal acquisition module NI-USB-4431 card.

2.2 Experimental results and discussion

Two types of absorbing porous materials, sponge and fiberglass, have been used in the absorbing material zone. The normalized acoustic impedances of sponge and fiberglass (relative to the acoustic impedance of air Z_0) calculated from the measured reflection coefficients are shown in Figure 4 as functions of frequency.

The measurements of the reflection coefficients, at frequencies from 500 Hz to 3000 Hz, for the box with inserted fiberglass and for the full QFAA (the quasi-periodic array of cylinders with fiberglass inserted) have been carried out. The results demonstrate (not shown here for brevity) that at the frequency ranges of 500 - 1581 Hz and of 2434 - 2745 Hz, the QFAA with fiberglass inserted provides lower reflection coefficient than the box with fiberglass inserted.

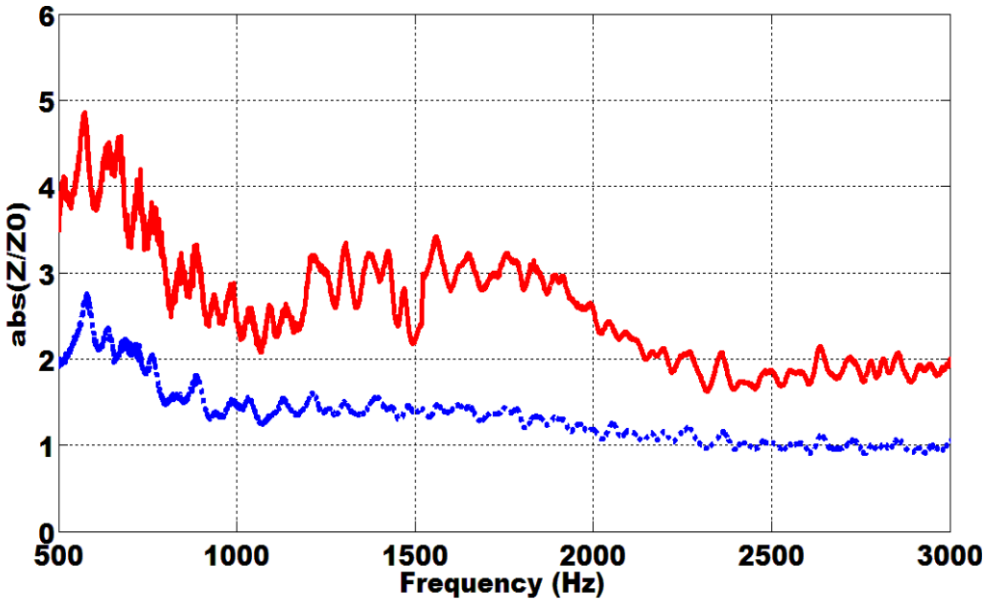

Figure 4: Normalised acoustic impedances of fiberglass (red line) and sponge (blue line) calculated from the measured reflection coefficients.

Although the above-mentioned results clearly demonstrate the benefit of using a matching metamaterial layer to reduce reflection, further substantial improvement can be made. In order to achieve better results, one needs to adjust the effective acoustic impedance at the exit of the metamaterial layer to make it as close as possible to the acoustic impedance of the inserted fiberglass. Therefore, it has been decided to remove a few last rows of Brass cylinders to reduce the effective impedance at the exit of the metamaterial layer and to get an adequate matching of the impedances. Two last rows have been removed, thus reducing the relative effective impedance at the exit of the matching metamaterial layer down to 2.4.

Measurement of the reflection coefficient have been carried out for the QFAA containing 11 and 10 rows of Brass cylinders, with fiberglass inserted. The results are shown in Figure 5 in comparison with the results for the box with fiberglass inserted, but in the absence of the metamaterial layer. It can be seen that at all frequencies the reflection coefficient for the box with fiberglass inserted is strongly reduced when the QFAA (with 10 rows of Brass cylinders and with fiberglass inserted) has been added. This demonstrates the functionality of matching the impedances using metamaterial layers. Namely, the device with 10 rows strongly outperforms the device with 12 and 11 rows in terms of the values of reflection coefficient. At frequencies above 750 Hz the values of reflection coefficient do not exceed 26 %. This means that at these frequencies the full QFAA with 10 rows of solid cylinders acts as an efficient acoustic absorber, with more than 93% of the impinging acoustic energy being absorbed.

Measurement of the reflection coefficient have been repeated for the full QFAA with sponge inserted for varying numbers of rows of Brass cylinders (10, 9, 8 and 7 rows). The results for 8 and 7 rows are shown in Figure 6 in comparison with the results for the box with sponge inserted, but in the absence of the metamaterial layer.

It can be seen that the lowest value of the reflection coefficient takes place for the QFAA with 7 rows. This is in agreement with Figure 2 showing that for 7 rows of cylinders the value of relative impedance of the metamaterial layer at the 7th row is about 1.5, which is close to the relative impedance of the sponge (see Figure 4). This demonstrates once again the functionality of impedance matching using metamaterial layers for enhancing the behaviour of acoustic absorbers.

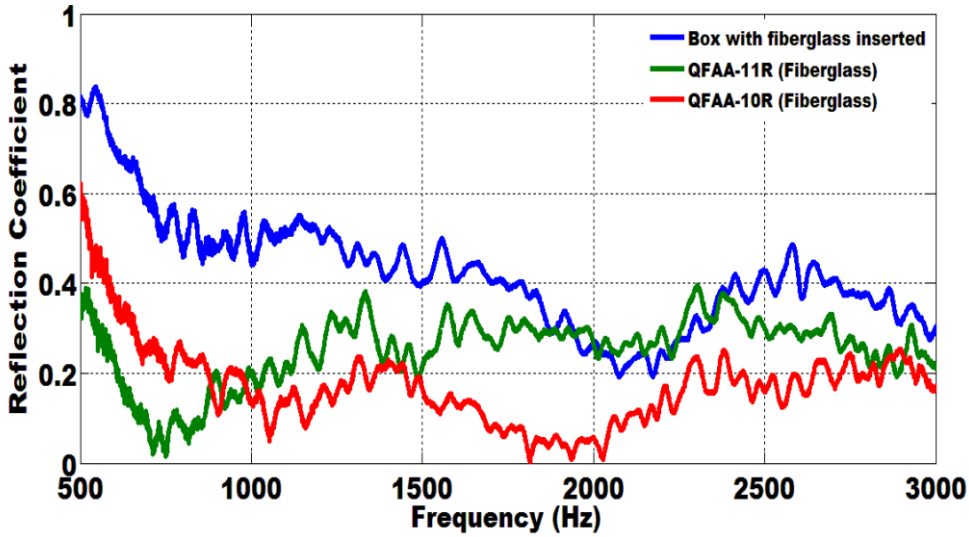

Figure 5: Sound reflection coefficients measured for the box with fiberglass inserted (blue line) and for the QFAA with 11 and 10 rows of Brass cylinders and fiberglass inserted (green and red lines respectively); measurements made using TFM method.

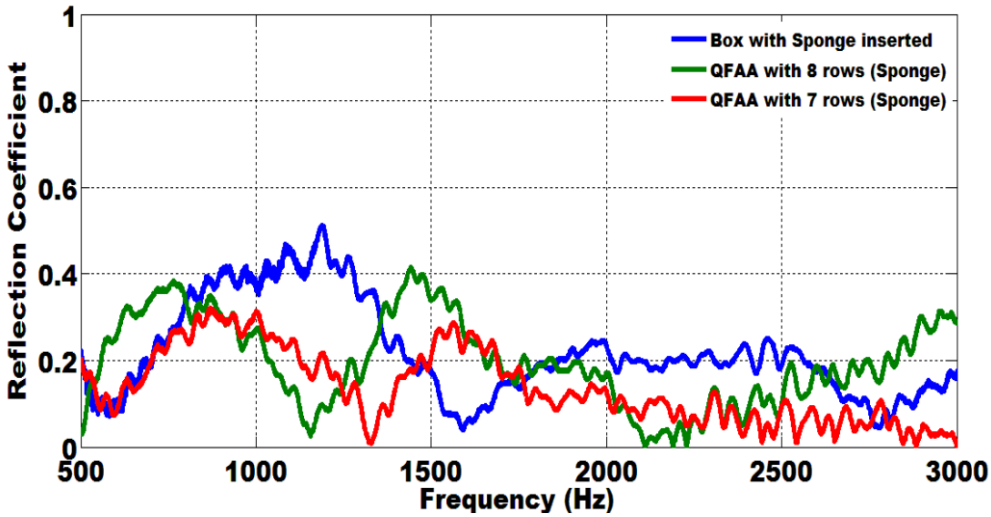

Figure 6: Sound reflection coefficients measured for the box with sponge inserted (blue line) and for the full QFAA with 8 and 7 rows of Brass cylinders and sponge inserted (green and red lines respectively); measurements made using TFM method.

It has been demonstrated in the above experiments that the values of sound reflection coefficient for the QFAA depend strongly on the impedance matching between the porous absorbing material and the exit of the gradient metamaterial layer. In particular, it has been shown that the QFAA with 10 rows of cylinders and with fiberglass as inserted absorbing material provides the lowest value of the reflection coefficient. This can be explained by a nearly perfect impedance matching achieved in this case. For the QFAA with sponge as inserted absorbing material, the lowest value of the reflection coefficient was observed for 7 rows of Brass cylinders, which again can be explained by a nearly perfect impedance matching in this case. The obtained results show that, for the quasi-flat geometrical configuration the presence of the impedance matching metamaterial layers in front of different porous absorbing material can bring a

substantial reduction in sound reflection coefficient in comparison with the case of reflection from the porous materials alone.

3 Acoustic black holes for sound absorption in air

In this section, we describe the investigations of the quasi-periodic structure that implements the acoustic black hole for sound absorption in air. 'Acoustic black holes' are relatively new physical and engineering objects that can absorb almost 100% of the incident wave energy. This makes them attractive for applications in noise and vibration control [4, 5, 11-20]. The principle of operation of acoustic black holes is based on a linear or higher order power-law-type decrease in velocity of the incident wave with propagation distance to almost zero, which should be accompanied by efficient energy absorption in the area of low velocity via small pieces of inserted absorbing materials.

So far, acoustic black holes have been investigated mainly for flexural waves in thin plates for which the required gradual reduction in wave velocity with distance can be easily achieved by changing the plate local thickness according to a power law, with the power-law exponent being equal or larger than two [4, 11-13]. This principle, in combination with adding small amounts of absorbing materials, has been applied to achieve efficient damping of flexural waves in plate-like structures using both one-dimensional 'acoustic black holes' (power-law wedges and beams with their sharp edges covered by narrow strips of absorbing materials) [4, 11-18] and two-dimensional 'acoustic black holes' (power-law-profiled pits with small pieces of absorbing materials attached in the middle), see e.g. [4, 5, 18, 19].

There are still very few investigations of acoustic black holes designed for absorption of sound in gases and liquids. Such acoustic black holes could be used to enhance acoustic absorption in traditional noise control. This would allow developers to apply smaller amounts of absorbing materials, which could reduce masses of the acoustic absorbing devices. The main difficulty here is to materialise a linear or higher order power-law decrease in velocity of the incident sound wave down to zero. Note in this connection that the recently developed acoustic absorbers based on gradient index metamaterials [6-10], in which no zero values of sound velocity were achieved, represent not acoustic black holes, but impedance matching absorbing devices (also see the previous section).

The first theoretical paper on acoustic black holes for sound absorption in air was published by Mironov and Pislyakov [21]. It was proposed in that paper to use inhomogeneous acoustic waveguides with walls of variable impedance materialised via quasi-periodic ribbed structures to achieve the required linear decrease in acoustic wave velocity with propagation distance down to zero. No inserted absorbing materials were considered in that theoretical paper. In what follows, we describe the results of our first experimental investigations of acoustic black holes for sound absorption in air, based on the above-mentioned inhomogeneous acoustic waveguides [22, 23].

3.1 Experimental samples

Based on the theory developed in the paper [21], two different samples of acoustic black holes formed by quasi-periodic ribbed structures materialising walls of variable impedance have been designed and manufactured - to provide linear and quadratic decreases in acoustic wave velocity with distance respectively.

The first structure, shown in Figure 7, has the waveguide inner radius described by a linear power law function of the distance *x:* $r(x) = \varepsilon_1 x$, it will be referred to as 'Linear Acoustic Black Hole' (LABH). The second structure has the inner radius as a quadratic power law function of *x:* $r(\mathrm{x}) = \varepsilon_2 \mathrm{x}^2$, it will be referred to as 'Quadratic Acoustic Black Hole' (QABH). Here ε_1 and ε_2 are constants. Both LABH and QABH consist of cylindrical plastic tubes of inner radius *R=115 mm* and length *L=255 mm* sealed at one end with a thick wooden backing of 13 mm thickness. Inside the tubes, a number of solid ribs (rings) of 2

mm thickness are mounted quasi-periodically, the first rib (ring) being separated from the wooden backing by the distance $S_b = 9\,mm$ (for LABH) and by the distance $S_b = 30\,mm$ (for QABH).

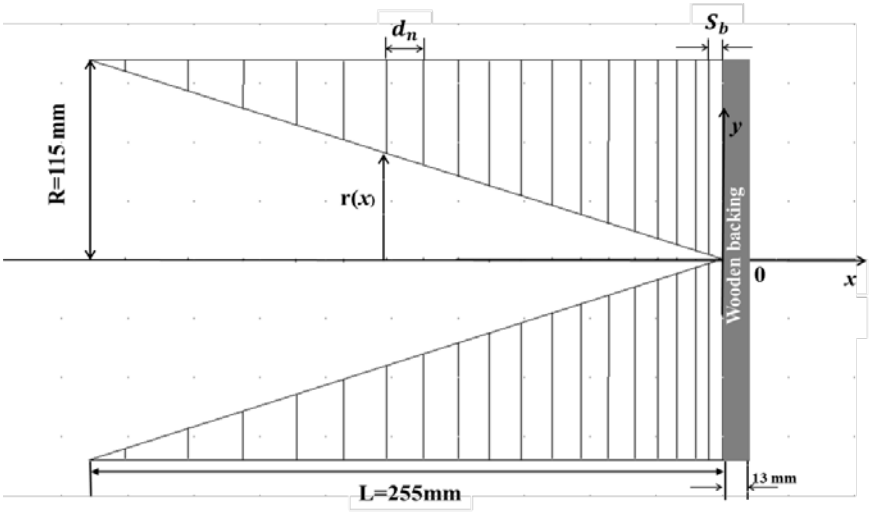

Figure 7: Schematic view of the manufactured Linear Acoustic Black Hole (LABH) showing the wooden backing and the distribution of the ribs whose inner radii decrease to almost zero.

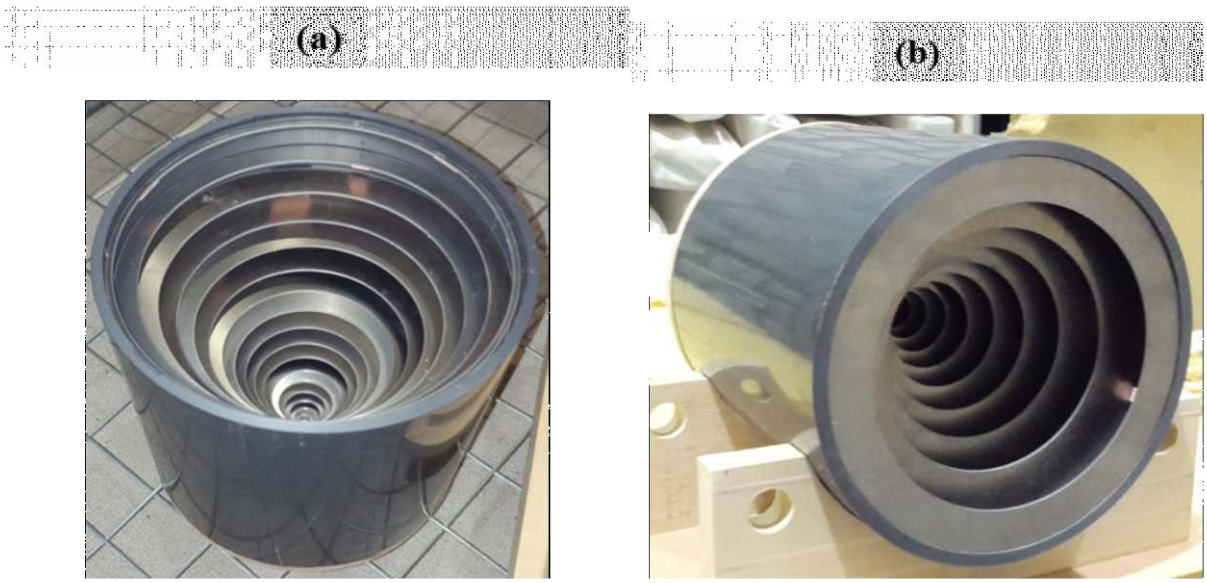

Figure 8: Photograph of LABH (a) and QABH (b).

The ribs (rings) have been made of laser cut steel in order to fit flush against the side of the tube wall, leaving no air gaps between the ribs' edges and the tube wall. The ribs for LABH and QABH were mounted with the increasing distances between them: $d_n = (3+n)\,mm$ and $d_n = (6+n)\,mm$ respectively, up to a maximum of 20 mm, where *n* is the rib number. These structures were expected to form the acoustic waveguides with varying wall admitances and varying cross sections. Inside the LABH

and QABH, there were 18 ribs and 14 ribs respectively. Photographs of LABH and QABH are shown in Figures 8(a) and 8(b) respectively.

3.2 Manufacturing of the matching impedance tube

Based on the two microphone transfer function method, according to the standard procedure detailed in ISO 10534-2 (see [24]), an impedance tube made of thick plastic has been designed and manufactured with the inner diameter close to those of the samples of acoustic black holes. This was done in order to measure the reflection coefficients of incident guided modes from the black holes only, and not from the jumps in tube diameters. The interior wall was smooth enough in order to maintain low sound attenuation for the lowest order guided modes (plane waves). A hard ring has been used to hold the black hole samples with the impedance tube. On the opposite end of the tube, a loudspeaker was fixed firmly, and an absorbent has been placed at the loudspeaker end of the tube to reduce the effect of resonances within the impedance tube. The length of the tube has to be long enough to ensure that plane waves are fully developed before reaching the microphones and the sample, and at least half of the longest wavelength can fit in it. Therefore, the length of the tube was $L_T = 1.5\ m$ and its inner diameter was $D_T = 225\ mm$.

Fourteen holes were drilled in the tube wall for positioning the measuring microphones, separated by 50 mm between them. The first hole was separated from one end of the tube by 50 mm. Those holes were drilled in order to enable measurements with different microphone positions and different separation between the input cross section of the sample and nearest microphone. Two holes have been used for positioning the microphones, the remaining holes had to be sealed in order to avoid air leakage into the tube. To achieve the low background noise, the tube must be sealed properly at all openings.

One of the important steps in using an impedance measurement tube is knowledge of the range of frequencies for which it will yield accurate results. Plane wave can be generated in a tube only if the excitation frequency is below the cut off frequency for the 2nd acoustic mode of the tube. This frequency can be determined as (see e.g. [25])

$$f_u = \frac{0.58c}{D_T}, \tag{3}$$

where c is the speed of sound, and D_T is the tube diameter. Thus, the upper limiting frequency for the tube parameters used was $f_u = 884\ Hz$.

There are also restrictions on the microphone spacing [25]. In particular, the lower limiting frequency depends on the distance between the microphone positions, S_0, which should be larger than 5 % of the longest measurable wavelength. Therefore, S_0 determines the lower limiting frequency f_l using the following condition:

$$f_l > \frac{0.05c}{S_0}. \tag{4}$$

Problems also rise, if the microphone spacing becomes too wide. This leads to an upper frequency limit due to microphone spacing given by:

$$f_u < \frac{0.45c}{S_0}. \tag{5}$$

For the selected distance $S_0 = 150\ mm$, it follows from (4) and (5) that $f_l > 114\ Hz$, and $f_u < 1092\ Hz$, the latter being larger than the above-determined $f_u = 884\ Hz$. Consequently, the useful frequency range for the constructed impedance tube is 114 – 884 Hz.

3.3 Experimental setup

The two microphone transfer function method (TFM) has been used in these experiments to measure the sound pressure reflection coefficients from the samples of the acoustic black holes. The experimental set-up comprised the impedance tube described above, a loudspeaker fixed at one end (it produced the constant broadband sound using a white noise generator), and two nominally identical microphones (GRAS 40E, pre-polarized ½ inch free-field). The two microphones were mounted flush with the inside wall of the tube, isolated from the tube to minimize sensitivity to vibration, and connected to a PC via a dynamic signal acquisition module NI-USB-4431 card (four analog input channels and one analog output channel) for making sound measurements. The selected spacing between the input cross section of the acoustic black holes and the nearest microphone and between the microphone positions were $L_0 = 200\,mm$ and $S_0 = 150\,mm$ respectively. Figure 9 shows the acoustic impedance tube with the microphones mounted on the tube. Shown are also the loudspeaker and the sample of acoustic black hole that is fixed to the end of the tube. The two microphone transfer function method was applied over a relatively large number of time samples, where the frequency response functions were processed to obtain the reflection coefficients from the two samples, LABH and QABH.

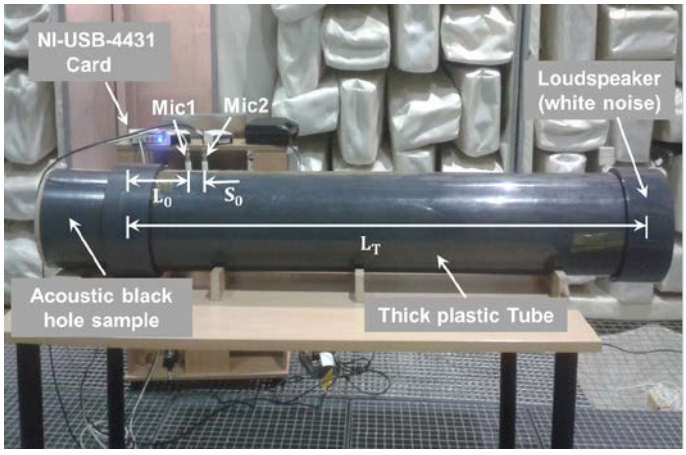

Figure 9: Photograph of the experimental set-up showing the impedance tube, two microphones mounted, a loudspeaker, the Acoustic black hole sample, and NI-USB-4431 Card: $L_T = 1.5\,m$, $D_T = 225\,mm$, $L_0 = 200\,mm$ and $S_0 = 150\,mm$.

3.4 Experimental results and discussion

Experimental measurements of the reflection coefficients for guided acoustic modes incident on the black holes (LABH and QABH) have been carried out in the frequency range of 100-1000 Hz. In the first instance, measurements were conducted without insertion of any absorbing materials. The results are shown in Figures 10 and 11 by solid blue lines. One can see significant reductions in the reflection coefficients for both acoustic black holes in the frequency range of 100-874 Hz. Note that this frequency range is within the useful frequency range of the constructed impedance tube. Comparison of the reflection coefficients results exhibited by LABH and QABH shows that the QABH is more efficient than LABH.

Following the ideas earlier successfully implemented in acoustic black holes for flexural waves [4, 5, 11-19], the additions of small pieces of sponge at the end of both samples have been made in attempts to

achieve further reduction in reflection coefficients [22]. The results indeed showed some reduction in the reflection coefficients when the sponge was covering the cavity occupied by the first four ribs of LABH. However, this reduction was not as large as it could be expected. Therefore, other types of inserted porous absorbing materials and their configurations had to be tested. In the later paper [23], two other types of absorbing material (fibreglass and mineral cotton) have been tested in both samples, covering the first four ribs. The results of the measurements of the reflection coefficients for both LABH and QABH are shown by dotted lines in Figures 10 and 11 respectively.

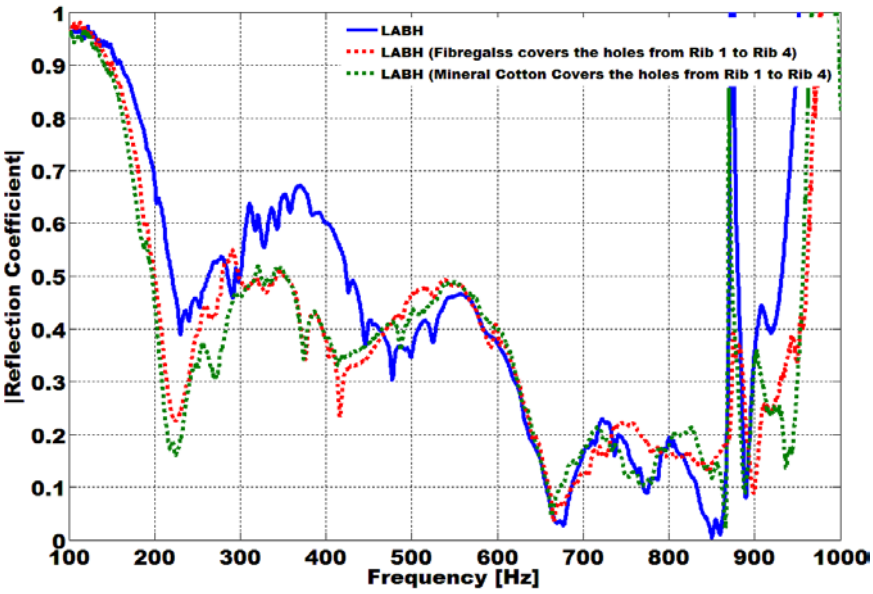

Figure 10: Frequency dependence of sound reflection coefficients from LABH (blue line), LABH (Fibreglass covers the holes of the first four ribs) (dashed red line), LABH (Mineral cotton covers the holes of the first four ribs) (dashed green line).

It can be seen from Figure 10 that the applied porous absorbing materials, fibreglass and mineral cotton, that cover the space containing the first four ribs of LABH, cause further reduction in the reflection coefficients in the frequency range of 100 – 465 Hz. Out of that range, it seems to be not much difference between LABH with and without absorbing porous materials inserted. In the case of QABH (see Figure 11), the curves of the reflection coefficients with and without inserted porous absorbing materials show similar behavior in the frequency range of interest.

Thus, it follows from the above results that the insertion of fibreglass and mineral cotton does not bring further significant reductions to the reflection coefficients for both samples. These rather modest results stimulated our attempts to use other configurations of absorbing materials to improve the efficiency of both devices in order to make it comparable with that for acoustic black holes for flexural waves.

For this purpose, two and four thin strips of sponge have been glued in opposite sides on the circumference of the first rib holes, with the aim of gradual increasing the sound absorption in the area of slow velocity [23]. The results of the measurements for both samples, LABH (two and four strips) and QABH (two and four strips), that are not shown here for shortness, have demonstrated that thin strips of sponge glued inside of both acoustic black holes do not produce noticeable reductions in the reflection coefficients, unlike in the case of acoustic black holes for flexural waves [4. 5, 11-19], where attachments of thin strips of absorbing materials result in dramatic reductions in flexural wave reflections.

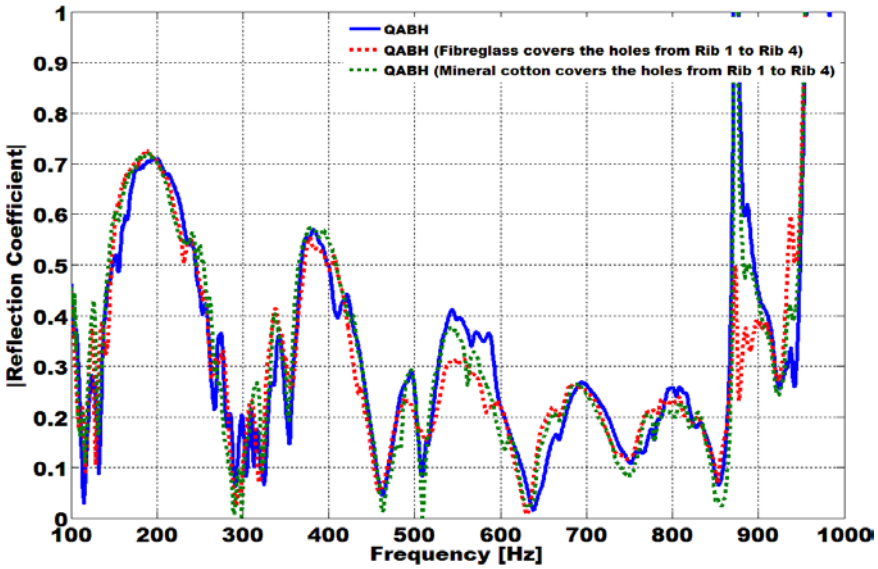

Figure 11: Frequency dependence of sound reflection coefficients from QABH (blue line), QABH (Fibreglass covers the holes of the first four ribs) (dashed red line), QABH (Mineral cotton covers the holes of the first four ribs) (dashed green line).

Thus, if both experimental black holes are used without inserted porous materials, they reduce the sound reflection coefficients, and their frequency behaviour generally agrees with the theoretical predictions [21]. However, the insertion of porous absorbing materials, sponge, fibreglass and mineral cotton, does not bring further noticeable reductions to the sound reflection coefficients. Combinations of two and four thin strips of sponge have been inserted in attempts to achieve a more 'gentle' increase in acoustic absorption with distance. However, these strip configurations also did not show significant reduction in the reflection coefficients.

4 Conclusions

It has been demonstrated experimentally that using gradient index metamaterial layers made of periodic arrays of solid cylinders can significantly reduce sound reflections from porous absorbing materials, resulting in the increased efficiency of sound absorption.

Values of the resulting sound reflection coefficient depend strongly on the impedance matching between the porous absorbing material and the exit of the gradient metamaterial layer. In particular, it has been shown that the metamaterial structure with 10 rows of cylinders and with fiberglass as inserted absorbing material provides the lowest value of the reflection coefficient. This can be explained by a nearly perfect impedance matching achieved in this case. For the metamaterial structure with sponge as inserted absorbing material, the lowest value of the reflection coefficient was observed for 7 rows of Brass cylinders, which again can be explained by a nearly perfect impedance matching in this case.

Experimental investigation of the two types of acoustic black holes for sound absorption in air have shown that, if both black holes are used without inserted porous materials, they reduce the sound reflection coefficients, and their frequency behaviour generally agrees with the theoretical predictions. However, the insertion of porous absorbing materials, sponge, fibreglass and mineral cotton, does not bring further noticeable reductions to the sound reflection coefficients, contrary to the expectations. Combinations of two and four strips of inserted sponge also did not show significant improvement.

Further theoretical and experimental inverstigations should be carried out to clarify these issues and to achieve lower values of sound reflection coefficients.

5 Acknowledgements

The research reported here has been supported by EPSRC grant EP/K038214/1.

6 References

[1] N. Engheta, R.W. Ziolkowski, *Metamaterials: physics and engineering explorations*, Wiley & Sons, Danvers (2006) (Chapter 1).

[2] V.G. Veselago, *The electrodynamics of substances with simultaneously negative values of ε and μ*, Soviet Physics - Uspekhi, Vol. 10, American Institute of Physics (1968), pp. 509-514.

[3] R.A. Shelby, D.R. Smith, S. Schultz, *Experimental verification of a negative index of refraction*, Science, Vol. 292 (2001), pp. 77-79.

[4] V.V. Krylov, *Acoustic black holes: Recent developments in the theory and applications*, IEEE Transactions on Ultrasonics, Ferroelectrics, and Frequency Control, Vol. 61, IEEE (2014), pp. 1296-1306.

[5] E.P. Bowyer, D.J. O'Boy, V.V. Krylov, F. Gautier, *Experimental investigation of damping flexural vibrations in plates containing tapered indentations of power-law profile*, Applied Acoustics, Vol. 74, Elsevier (2013), pp. 553–560.

[6] R. Li, X. Zhu, B. Liang, Y. Li, X. Zou, J. Cheng, *A broadband acoustic omnidirectional absorber comprising positive index materials*, Applied Physics Letters, Vol. 99, American Institute of Physics (2011), pp. 193507.

[7] A. Climente, D. Torrent, J. Sanchez-Deseha, *Omnidirectional broadband acoustic absorber based on metamaterials*, Applied Physics Letters, Vol. 100, American Institute of Physics (2012), pp. 144103.

[8] O. Umnova, B. Zajamsek, *Omnidirectional graded index sound absorber*, Proceedings of the international conference 'Acoustics 2012', Nantes, France, pp. 3631-3637.

[9] A. Azbaid El Ouahabi, V.V. Krylov, D.J. O'Boy, *Quasi-flat acoustic absorber enhanced by metamaterials*, Proceedings of Meetings on Acoustics, Vol. 22, Acoustical Society of America (2014), pp. 040002.

[10] A. Azbaid El Ouahabi, V.V. Krylov, D.J. O'Boy, *Gradient metamaterial layers as impedance matching devices for efficient sound absorption*, Proceedings of the 10th European Congress and Exposition on Noise Control Engineering (EuroNoise 2015), Maastricht, The Netherlands, 31st May - 3rd June 2015, pp.989-994.

[11] V.V. Krylov, New type of vibration dampers utilising the effect of acoustic ‘black holes’, Acta Acustica united with Acustica, **90**(5), 830–837, (2004).

[12] V.V. Krylov, F.J.B.S. Tilman, *Acoustic ‘black holes’ for flexural waves as effective vibration dampers*, Journal of Sound and Vibration, Vol. 274, Elsevier (2004), pp. 605-619.

[13] V.V. Krylov, R.E.T.B. Winward, *Experimental investigation of the acoustic black hole effect for flexural waves in tapered plates*, Journal of Sound and Vibration, Vol. 300, Elsevier (2007), pp. 43-39.

[14] V. Kralovic, V.V. Krylov, *Damping of flexural vibrations in tapered rods of power-law profile: Experimental studies*, Proceedings of the Institute of Acoustics, Vol. 29, No. 5, Institute of Acoustics (2007), pp. 66-73.

[15] D.J. O'Boy, V.V. Krylov, V. Kralovic, *Damping of flexural vibrations in rectangular plates using the acoustic black hole effect*, Journal of Sound and Vibration, Vol. 329, Elsevier (2010), pp. 4672–4688.

[16] J.J. Bayod, *Experimental study of vibration damping in a modified elastic wedge of power-law profile*, Journal of Vibration and Acoustics, Vol. 133 (2011), pp. 061003.

[17] V. Denis, A. Pelat, F. Gautier, B. Elie, Modal Overlap Factor of a beam with an acoustic black hole termination, Journal of Sound and Vibration, Vol. 333, Elsevier (2014), pp. 2475-2488.

[18] V.B. Georgiev, J. Cuenca, F. Gautier, L. Simon, V.V. Krylov, *Damping of structural vibrations in beams and elliptical plates using the acoustic black hole effect*, Journal of Sound and Vibration, Vol. 330, Elsevier (2011), pp. 2497–2508.

[19] S.C. Conlon, J.B. Fahnline, F. Semperlotti, *Numerical analysis of the vibroacoustic properties of plates with embedded grids of acoustic black holes*, Journal of the Acoustical Society of America, Vol. 137, No. 1, American Institute of Physics (2015), pp. 447-457.

[20] M.A. Mironov, *Propagation of a flexural wave in a plate whose thickness decreases smoothly to zero in a finite interval*, Soviet Physics – Acoustics, Vol. 34, American Institute of Physics (1988), pp. 318-319.

[21] M.A. Mironov, V.V. Pislyakov, *One-dimensional acoustic waves in retarding structures with propagation velocity tending to zero*, Acoustical Physics, Vol. 48, No. 3, Springer (2002), pp. 347–352.

[22] A. Azbaid El-Ouahabi, V.V. Krylov, D.J. O'Boy, *Experimental investigation of the acoustic black hole for sound absorption in air*, Proceedings of the 22nd International Congress on Sound and Vibration (ICSV 2015), Florence, Italy, 12-16 July 2015, 8 pp.

[23] A. Azbaid El-Ouahabi, V.V. Krylov, D.J. O'Boy, *Investigation of the acoustic black hole termination for sound waves propagating in cylindrical waveguides*, Proceedings of the 44th International Congress and Exposition on Noise Control Engineering (InterNoise 2015), San Francisco, USA, 9-12 August 2015, 10 pp.

[24] ISO 10534-2, *Acoustics – Determination of sound absorption coefficient and impedance in impedance tube – Part 2: Transfer-function method*, International Standard Organisation (1998).

[25] T.J. Cox, P.D'Antonio, *Acoustic absorbers and diffusers: Theory, design and application*, 2nd Edition, Taylor & Francis, Oxford (2009).